TECHNICAL REPORT
NATICK/TR-03/003

AD_____

DRAWING BEHAVIOR OF ULTRAHIGH MOLECULAR WEIGHT POLYETHYLENE (UHMWPE) FIBERS IN SUPERCRITICAL CO_2

by
Alan J. Lesser

University of Massachusetts
Amherst, MA 01003-4530

November 2002

Final Report
July 2000 - July 2001

Prepared for
U.S. Army Soldier and Biological Chemical Command
Soldier Systems Center
Natick, Massachusetts 01760-5019

REPORT DOCUMENTATION PAGE

Form Approved
OMB No. 0704-0188

1. REPORT DATE *(DD-MM-YYYY)*	2. REPORT TYPE	3. DATES COVERED *(From - To)*
04-11-2002	Final	July 2000 - July 2001

4. TITLE AND SUBTITLE
DRAWING BEHAVIOR OF ULTRAHIGH MOLECULAR WEIGHT POLYETHYLENE (UHMWPE) FIBERS IN SUPERCRITICAL CO2

5a. CONTRACT NUMBER
DAAD16-00-P-0769

5b. GRANT NUMBER

5c. PROGRAM ELEMENT NUMBER

6. AUTHOR(S)
Alan J. Lesser

5d. PROJECT NUMBER

5e. TASK NUMBER

5f. WORK UNIT NUMBER

7. PERFORMING ORGANIZATION NAME(S) AND ADDRESS(ES)
Polymer Science & Engineering Dept.,
University of Massachusetts
Amherst, MA 01003-4530

8. PERFORMING ORGANIZATION REPORT NUMBER
5-28101

9. SPONSORING/MONITORING AGENCY NAME(S) AND ADDRESS(ES)
U.S. Army Soldier & Biological Chemical Command
Soldier Systems Center
ATTN: AMSSB-RIP-B(N)
Natick, MA 01760-5019

10. SPONSOR/MONITOR'S ACRONYM(S)

11. SPONSOR/MONITOR'S REPORT NUMBER(S)
NATICK/TR-03/003

12. DISTRIBUTION/AVAILABILITY STATEMENT
Approved for public release; distribution is unlimited

13. SUPPLEMENTARY NOTES

14. ABSTRACT
The drawing behavior of Ultrahigh Molecular Weight Polyethylene (UHMWPE) fibers in supercritical CO2 (scCO2) is compared to that in air at different temperatures. Temperature substantially influences the drawing properties in air, while in scCO2 a constant draw stress and tensile strength are observed. Differential Scanning Calorimetry (DSC) shows an apparent development of a hexagonal phase along with significant improvements in crystallinity of air-drawn samples with increasing temperature. The existence of this phase is not confirmed by Wide Angle X-ray Scattering (WAXS) showing that air-drawn samples crystallize in an internally constrained manner. In contrast, scCO2 allows crystals to grow without constraints through a possible crystal-crystal transformation, increasing the processing temperature to 110°C.

15. SUBJECT TERMS
UHMWPE (ULTRA HIGH MOLECULAR WEIGHT POLYETHYLENE) POLYMERIC MATERIALS
SUPERCRITICAL CO2 TENSILE STRESS FIBERS
AIR DRAWING MECHANICAL PROPERTIES DRAWING BEHAVIOR
DEFORMATION

16. SECURITY CLASSIFICATION OF:			17. LIMITATION OF ABSTRACT	18. NUMBER OF PAGES	19a. NAME OF RESPONSIBLE PERSON
a. REPORT	b. ABSTRACT	c. THIS PAGE			John W. Song
U	U	U	SAR	33	19b. TELEPHONE NUMBER *(Include area code)* 508-233-5531

Table of Contents

List of Figures

List of Tables

Preface

The drawing behavior of Ultra High Molecular Weight Polyethylene (UHMWPE) fibers in supercritical CO_2 ($scCO_2$) is compared to that in air at different temperatures. Temperature substantially influences the drawing properties in air, while in $scCO_2$ a constant draw stress and tensile strength are observed. Differential Scanning Calorimetry (DSC) shows an apparent development of a hexagonal phase along with significant improvements in crystallinity of air-drawn samples with increasing temperature. The existence of this phase is not confirmed by Wide Angle X-ray Scattering (WAXS) showing that air-drawn samples crystallize in an internally constrained manner. In contrast, $scCO_2$ allows crystals to grow without constraints through a possible crystal-crystal transformation, increasing the processing temperature to 110°C.

This report was prepared under Contract No. DAAD16-00-P-0769 and reflects the results of an investigation performed during the period July 2000 to July 2001 by Alan J. Lesser, associate professor at the Polymer Science and Engineering Dept., University of Massachusetts, Amherst, MA 01003.

DRAWING BEHAVIOR OF ULTRAHIGH MOLECULAR WEIGHT POLYETHYLENE (UHMWPE) FIBERS IN SUPERCRITICAL CO_2

INTRODUCTION

Introducing supercritical CO_2 into the drawing process of a polymeric material can modify its final properties. The presence of supercritical CO_2 promotes changes in the state of stress of drawing, imposing hydrostatic contributions to the principal stress of uniaxial deformation, creating a very complex state of stress that in some cases is able to modify the physical and mechanical properties of the deformed material. Factors due to the presence of supercritical CO_2 are combined in a complex way with those related with the imposed hydrostatic pressure. The complexity of this process is enhanced by the fact that the properties of CO_2 are highly pressure- and temperature- dependent. Supercritical CO_2 as described elsewhere is a non-solvent for most polymers, with the exception of some fluoropolymers. It is widely accepted that supercritical CO_2 selectively permeates the amorphous phase of a semi-crystalline polymer inducing crystallization. Supercritical CO_2 has also been described as a reversible plasticizer since it is easily removed from the system simply by releasing the pressure, leaving the final product solvent-free, reducing the costs of solvent removal.

The imposed hydrostatic pressure has been related with some changes observed experimentally as well. Crystal-crystal transitions have been observed in the case of polymorphic materials when a high-pressure medium is imposed. Along with this, it is well known that in some cases, high-pressure tend to suppress chain mobility as well as to enhance the draw efficiency of a process.

Hobbs and Lesser[1] have shown that the final properties of Poly(ethylene terephthalate) (PET) fibers drawn by a two-stage process were considerably affected by the presence of CO_2. The CO_2 pressure dramatically affected the drawing behavior during the first stage as well as the total draw ratio obtained at the end of the second stage. A 10% increase in modulus and strength was observed for the case of samples treated in high pressure CO_2. This behavior has been proved to be valid by Lesser in other semi-crystalline polymers as well. Considerable improvements in the ultimate tensile stress, as well as in the young modulus for the case of Nylon 6,6 fibers when drawn in the presence of supercritical CO_2 (2500 psi) have been observed. Significant increases in crystallinity and crystalline orientation have been estimated for these fibers when treated in CO_2.

EXPERIMENTAL

Materials

The UHMWPE fibers (Spectra® 900) obtained from John Song at U.S. Army Soldier Systems Command—RD&E Center at Natick, Massachusetts have been used in this study. The intrinsic properties of these fibers, as reported commercially, are summarized in Table 1. The ultra high purity carbon dioxide (CO_2) used in this study was obtained from Merriam Graves Co.

Table 1. Physical properties of UHMWPE fibers used in this study.

Weight/Unit length (Denier)	1200
Ultimate Tensile Strength (GPa)	2.57
Breaking Strength (lbs)	95.2
Modulus (GPa)	62
Elongation (%)	3.6
Density (g/cc)	0.97
Filament/tow	120

Apparatus and Sample Preparation

The drawing experiments were conducted using an originally designed apparatus shown in Figure 1. The apparatus is mounted on a universal tensile testing machine (Instron Model® 1333) and it is constructed primarily of standard high-pressure fittings.

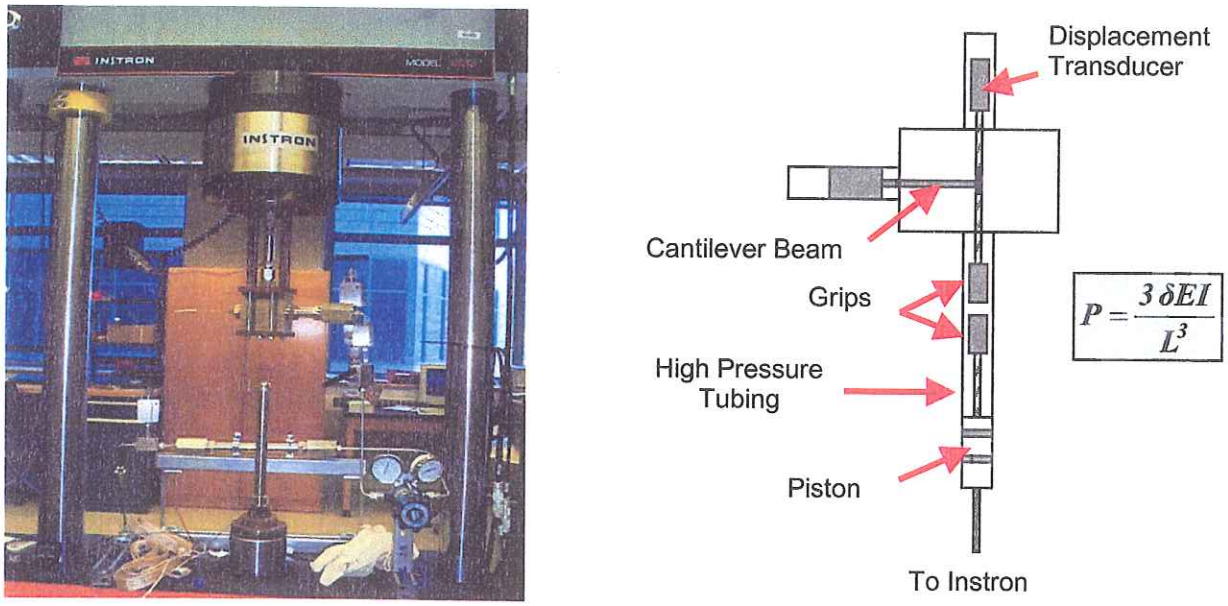

Figure 1. High-pressure drawing apparatus.

The design is capable of making in situ force measurements using a calibrated stainless steel cantilever beam and a linear variable displacement transducer (LVDT) with electronics located outside the high-pressure medium. As depicted in Figure 1, the mechanical grips are located inside a high-pressure vessel and directly attached to the movable piston of the Instron.

A high-pressure carbon dioxide pump (Hydro-Pac, Inc.) with a maximum discharge pressure of 30,000 psi is used to introduce CO_2 to the system. Specific control over the pressure was maintained during the entire experiment. The electronic signals and crosshead displacements are monitored via a personal computer using MTS Teststar II® software. The initial cross-sectional area was determined both by using SEM images of the tested material and by the linear density of the fibers and the density of the undrawn UHMWPE fiber (0.97 g/cm^3) as reported in Table1. Strain is calculated from the relative displacement between the crosshead and the beam divided by the original fiber gauge length. Draw ratios were estimated from the strain measurements and by external marks placed in the specimen prior to the deformation. All the drawing experiments were conducted at a strain rate of 10mm/min and the gauge length of the samples was always maintained at 60mm ± 5mm.

Single filament tests were performed on an Instron 1123® universal testing machine, using a 2000 lbs load cell. Specimens of 20 mm ± 2mm were cut and the experiments were always conducted at a strain rate of 10%/min (≈2mm/min). All the mechanical properties reported here (Tensile strength, elastic modulus and break strain) were obtained from 10+ specimens. Due to the negligible adhesion of UHMWPE fibers to commercially available epoxy adhesives, a special mechanical grip was designed for these measurements. The fiber diameter was measured using either a high magnification optical microscope calibrated with a micrometer scale or by the corresponding SEM images of the tested specimen.

RESULTS AND DISCUSSION

Mechanical Properties: Bundle and single fiber tests

Bundle Tests

A typical drawing behavior for the samples studied here is depicted in Figure 2. From this figure, it is easy to recognize some of the general variables observed during the drawing of UHMWPE using the apparatus described before. Four variables are employed to describe the deformation of a UHMWPE sample from the raw data. A typical elastic region, where the amount of deformation or strain is directly proportional to the imposed stress, is observed in all the experiments. In this region it is clear that all the filaments in the bundle (a total of 120) are deformed homogeneously, i.e. they carry the same amount of load. The limit of this elastic region is described by two variables, the amount of strain obtained at this point (ε_f) and the level of stress attained at this deformation (σ_f). The point (ε_f,σ_f) describes the moment during the deformation at which the first filament of the bundle fails. After this occurs, subsequent failure of a certain number of filaments in the bundle is observed at different levels of stress, describing a chaotic behavior up to a

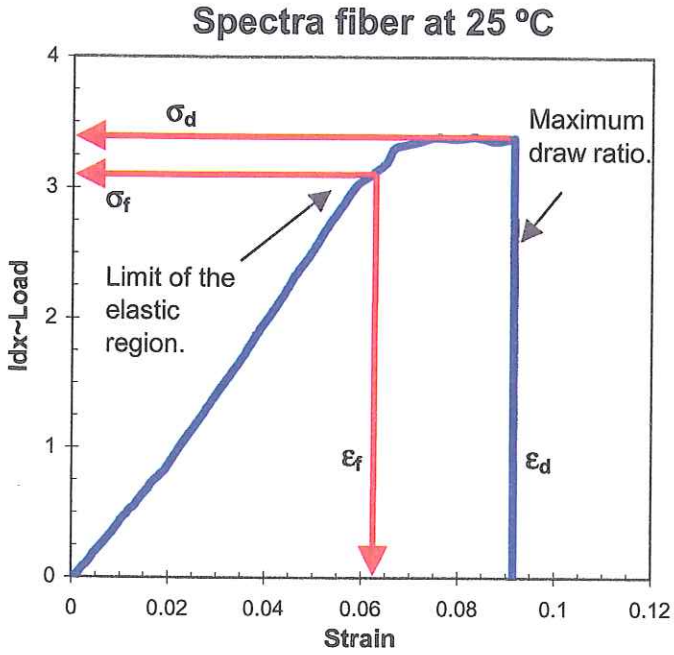

Figure 2. Typical drawing behavior of an UHMWPE fiber.

certain value of stress (σ_d), where no more independent filament failure is observed. The quantity σ_d, defined as the draw stress, represents the level of stress at which the remaining filaments in the bundle are homogeneously deformed up to a strain (ε_f), which describes the amount of deformation obtained by the sample prior to a catastrophic failure. The value of (ε_f) is used to estimate the maximum draw ratio obtained in the sample.

As described before, the drawing behavior of samples treated in the presence of high-pressure CO_2 (3000 psi) is compared with that observed at ambient pressures within a certain temperature range. As shown in Figures 3 and 4, the drawing behavior is completely modified by the introduction of high-pressure CO_2 into the system.

The drawing behavior in air is very temperature dependent as can be seen in Figure 3. It is easy to recognize that by increasing the drawing temperature, the apparent modulus is substantially decreased, as judged by the slope at smaller strains within the elastic region. Along with this, a clear decrease in the draw stress (σ_d) is observed with increasing temperature. It is convenient to point out at this moment that for the case of air-drawn samples, a maximum processing temperature of 80°C is clearly determined. Beyond this temperature, considerable softening of the material is observed, something that correlates very well with the appearance of a α-transition in UHMWPE at this temperature. It is widely known that depending on the crystallization process and the amount of orientation in the sample this transition can be detected in a wide temperature range. For this type of fibers due to the high orientation and crystallinity, the α-transition

is located in a rather small temperature range (80-83°C). The α-transition will involve the movements of polymer chains within the crystals; something that as observed experimentally will destroy completely the mechanical integrity of the fiber.

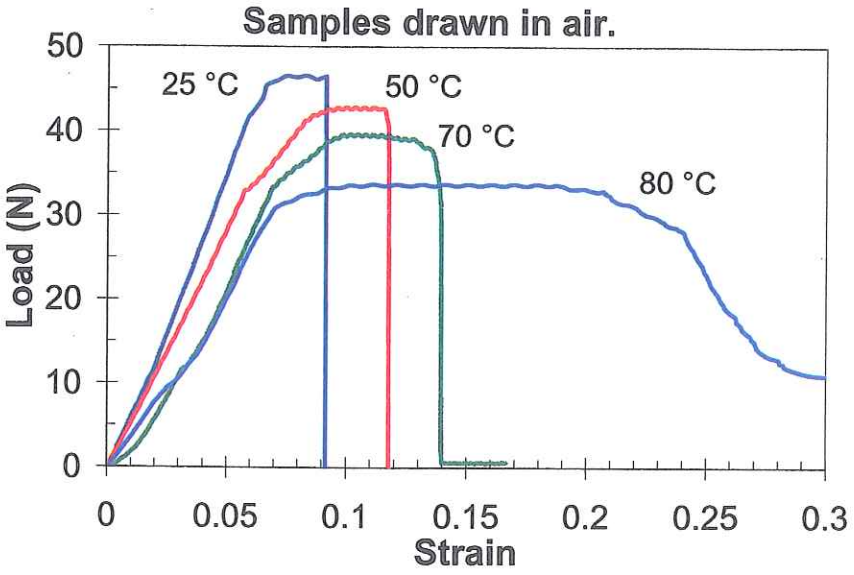

Figure 3. Drawing behavior of UHMWPE fibers deformed in air at different temperatures.

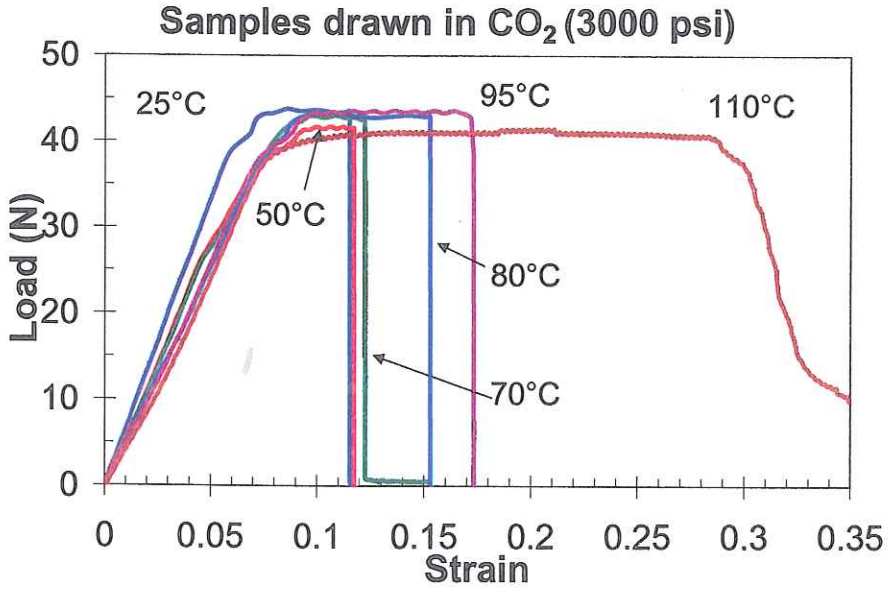

Figure 4. Drawing behavior of UHMWPE fibers deformed in the presence of CO_2 at different temperatures.

This behavior is very different to that observed in the presence of high-pressure CO_2, as can be seen in Figure 4. In this case an increase in the drawing temperature do

not affect considerably the apparent modulus, i.e. a constant slope is observed at small strains regardless of the processing temperature. The draw stress (σ_d) also remains unaffected with increasing temperature.

From Figure 4 it is clear that the temperature dependence observed for the case of the air-drawn samples is completely suppressed by introducing CO_2. Another important observation is that in this case the processing range has been increased up to a temperature of 110°C. A 30°C increase in the processing range is obtained when the deformation is done in the presence of supercritical CO_2, without significant softening of the material. This observation suggests that either the presence of CO_2 or the imposed hydrostatic pressure suppress the α-transition, shifting it to higher temperatures and allowing the extension of the processing range for UHMWPE fibers.

A quantitative description of the four variables used to describe the drawing behavior of samples treated at different processing conditions can be found in the following figures. Figure 5 describes the temperature dependence of the draw stress (σ_d)

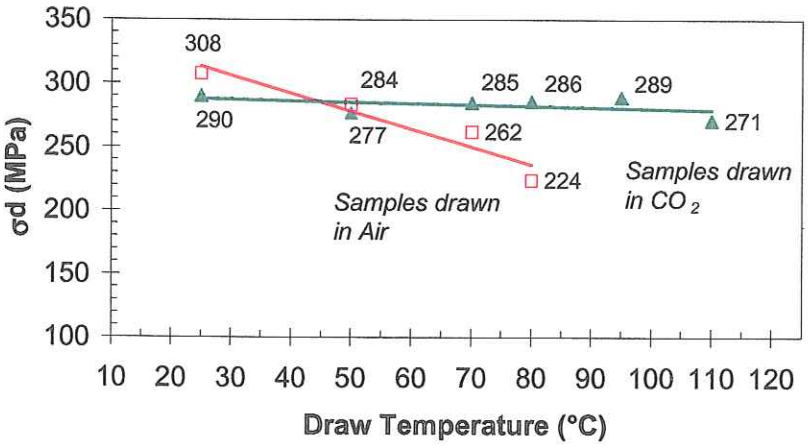

Figure 5. Draw Stress σ_d of UHMWPE fibers deformed at different processing conditions.

for the case of air-drawn samples, going from a value of 308 MPa at 25°C to a value of 224 MPa at 80°C, which as described before represents the limiting temperature in this case. In contrast, the behavior in the presence of CO_2 as can be seen in the same figure, remains constant at a value of 286 MPa over the entire range.

The maximum draw ratio estimated from ε_d is depicted in Figure 6. As can be seen in this figure, the maximum draw ratio increases in a significant way with increasing temperature. The maximum deformation (1.35) was obtained by a sample processed in supercritical CO_2 at the highest temperature (110°C). However, as a general trend, it can be seen that higher deformations are obtained when the experiment is conducted without CO_2, a clear indication that the mechanical properties are maintained by processing the sample in CO_2. In the range of 25-80°C, clear temperature dependence is present for the case of air-drawn samples while slight changes in the draw ratio are observed for the case of the samples drawn in high-pressure CO_2.

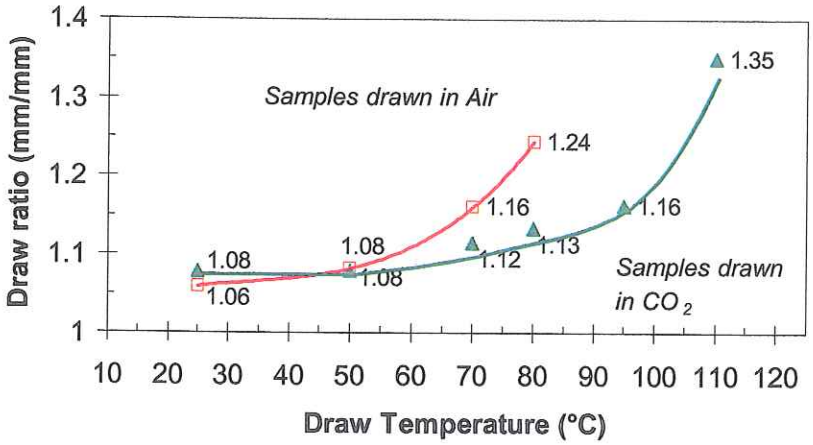

Figure 6. Maximum Draw Ratios of UHMWPE fibers deformed at different processing conditions.

The initial elastic region is described quantitatively in Figures 7 and 8. No changes in σ_f are observed when processing the sample in the presence of CO_2 as shown in Figure 7. A constant value of 255 MPa is observed in this case along the entire processing range. In contrast, a clear temperature dependence is observed for the case of air-drawn samples.

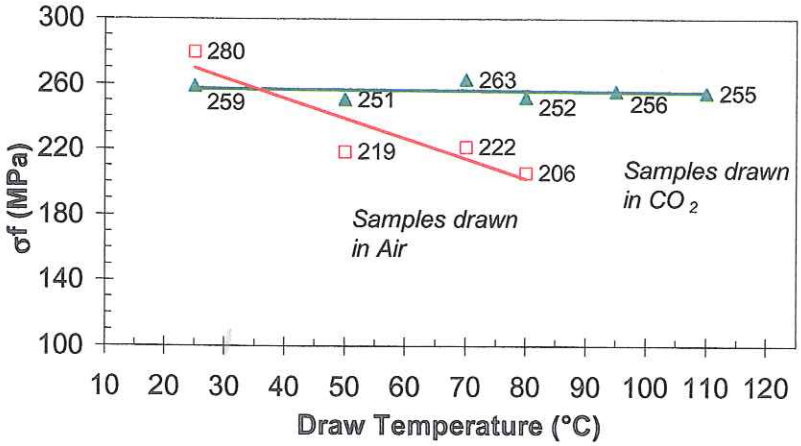

Figure 7. σ_f of UHMWPE fibers deformed at different processing conditions.

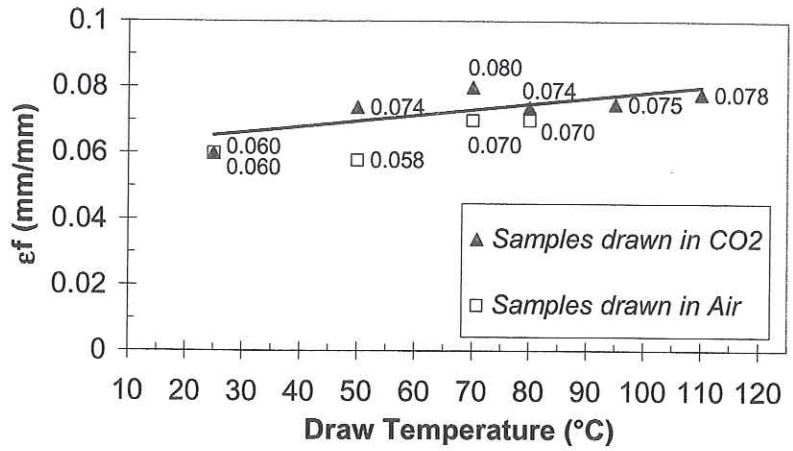

Figure 8. ε_f of UHMWPE fibers deformed at different processing conditions.

The level of stress at which the first filament of the bundle breaks is decreased considerably in this case, from a value of 280 MPa at 25°C to 206 MPa at 80°C. Surprisingly, the level of strain at which the elastic region ends (ε_f) appears to be independent of the processing conditions as can be seen in Figure 8. The drawing temperature, as judged from Figure 8, appears to have a predominant effect upon the value of ε_f. Apparently, both the hydrostatic pressure and the presence of CO_2 do not have a significant effect on ε_f.

Single Fiber Tests

As described in the experimental section, the mechanical properties of the drawn materials were determined using an Instron testing machine model 1123. Typically 10+ 20mm gauge length specimens were tested at a strain rate of 2mm/min. A representative experiment was then chosen to estimate the mechanical properties of the fiber. Due to the negligible adhesion of UHMWPE fibers to commercially available epoxy adhesives a special mechanical grip was designed for this measurements. The original design of the mechanical grip prevents any slippage of the fiber during the deformation, giving fairly good experimental results.

Again samples treated at different processing conditions were compared in terms of their inherent mechanical properties. Elastic modulus, strain at break and break stress or tensile strength were measured from the representative experiment of every set. Some of the results are plotted in Figure 9.

In Figure 9 the results obtained for the undrawn UHMWPE fiber is also included for comparison. It is clear from this figure that the mechanical response did not change in a significant manner by increasing temperature for samples treated in the presence of high-pressure CO_2. Almost the same behavior is described at small strains for fibers treated at 25°C and 95°C that were treated in high-pressure CO_2. This is another indication of the fact that the high-pressure environment created by the introduction of

supercritical CO_2 helps to maintain the integrity of the fiber, without any alteration of their mechanical properties.

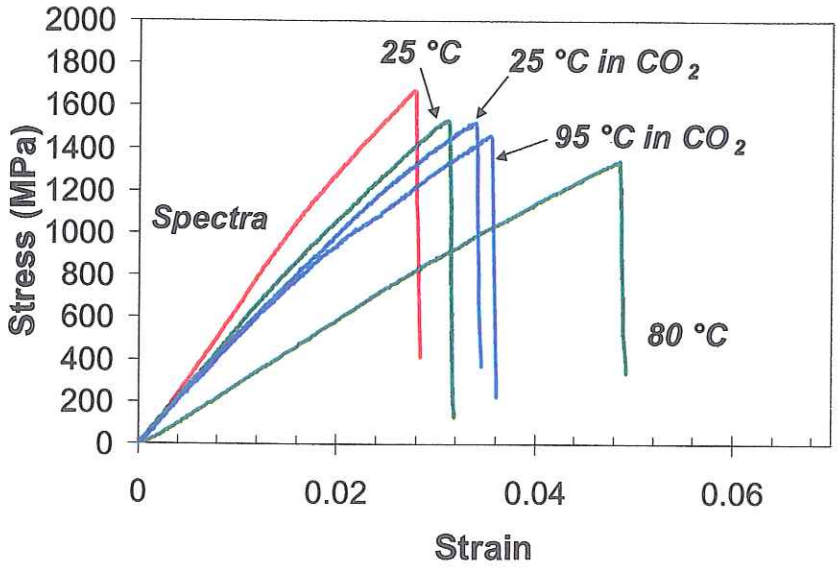

Figure 9. Single fiber tests of some of the UHMWPE fibers treated at different processing conditions.

However, as seen in Figure 9, the behavior for the air-drawn samples is completely different. Samples drawn at different conditions present a totally different mechanical response. Again, a temperature dependence on the mechanical properties is observed for the case of air-drawn samples. Both the elastic modulus and the tensile strength are considerably reduced by increasing the drawing temperature from 25°C to 80°C. A quantitative view of these results can be obtained from Table 2.

Table 2. Single fiber tests of some of the UHMWPE fibers treated at different processing conditions.

Sample	Modulus (GPa)	Strain at break (%)	Break stress (MPa)
Undrawn Spectra	69.91	2.7	1671.6
25 °C in Air	55.39	3.15	1528.12
25 °C in CO_2	52.40	3.4	1522.09
80 °C in Air	30.83	4.7	1334.10
95 °C in CO_2	48.85	3.57	1452.27

From this table it can be seen that almost a 45% decrease in the elastic modulus along with a 13% reduction in tensile strength is observed by increasing the processing temperature from 25°C to 80°C for the case of the air-drawn samples. In contrast, only negligible reductions in elastic modulus and tensile strength (<7%) are observed, when

the sample is treated in CO_2 even at a higher processing temperature (95°C). However, in all cases it seems that the macroscopic deformation imposed to the samples have promoted an overall decrease in the mechanical properties when compared to the undrawn sample. This reduction for the case of CO_2-drawn samples is compensated by the fact that the processing range, as described before, has been increased in a considerable manner.

The complete set of results for the mechanical properties of fibers treated at different conditions are presented in Figures 10, 11 and 12.

Figure 10 illustrates the fact that the elastic modulus remains unchanged over the entire temperature range, when processing the fiber in high-pressure CO_2. Samples treated in air, however, show a considerable decrease in elastic modulus with increasing temperature. This temperature dependence becomes more important at higher temperatures, showing that the fiber becomes weaker and weaker when drawn in air at elevated temperatures.

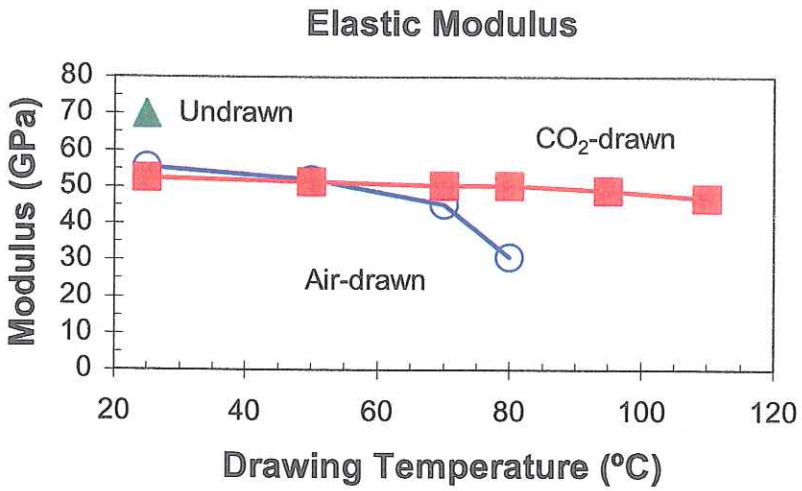

Figure 10. Elastic Modulus of UHMWPE fibers treated at different processing conditions.

A similar behavior is observed for the strain at break, as can be seen in Figure 11. No temperature dependence is observed when the sample is treated with CO_2, showing that the mechanical integrity of the sample is maintained and the required macroscopic deformation to break the sample remains unaltered regardless of the processing conditions. The behavior for air-drawn samples is again different. Larger deformations can be obtained for samples processed at a higher temperature. This temperature dependence, as for the case of the elastic modulus, becomes more important at higher temperatures, and it might be related with the observed decrease in the elastic modulus.

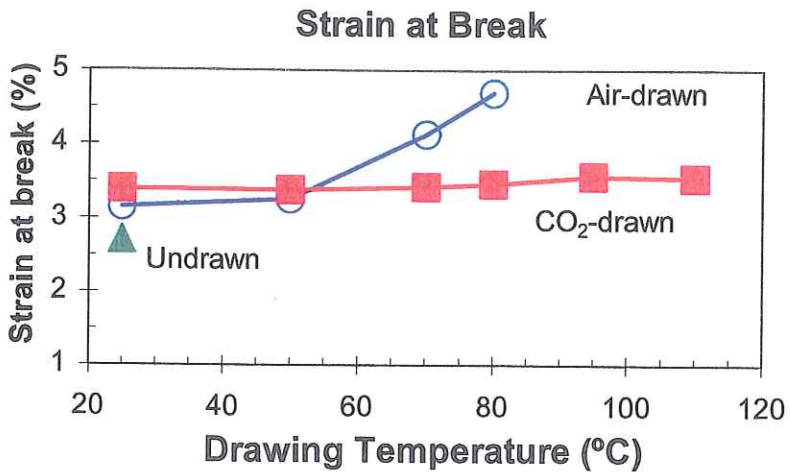

Figure 11. Strain at break of UHMWPE fibers treated at different processing conditions.

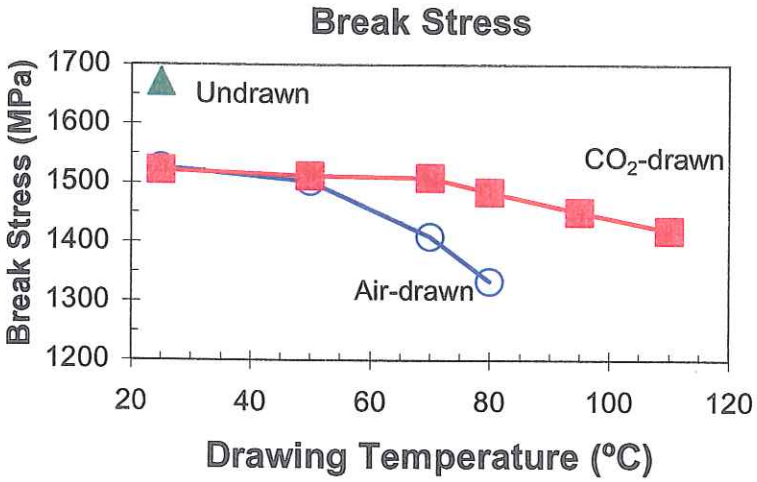

Figure 12. Break Stress or Tensile Strength of UHMWPE fibers treated at different processing conditions.

The observation that a UHMWPE fiber maintains its mechanical properties when drawn in the presence of high-pressure CO_2 is also supported in Figure 12. Again no significant changes in the tensile strength for fiber drawn in CO_2 at different temperatures are observed. Figure 12 also show a strong temperature dependence for air-drawn samples processed at different temperatures. As mentioned before, the tensile strength of undrawn sample is higher, showing that the drawing process has promoted a slight decrease in the mechanical properties. As pointed out before, this decrease, that for the case of CO_2-drawn samples corresponds to less than 9%, could not be of importance considering that the processing temperature range has been increased in this case by at least 30°C.

Differential Scanning Calorimetry (DSC)

Differential Scanning Calorimetry (DSC) was employed to analyze the thermal behavior of samples processed at different conditions. DSC experiments were performed in a TA Instruments thermal analyst model 2100. DSC experiments were conducted in the temperature range of 25-210°C at a moderately slow heating rate (1°C/min) in order to obtain quantitative differences of the thermal response of each sample. A typical DSC scan of an undrawn UHMWPE fiber is shown in Figure 13.

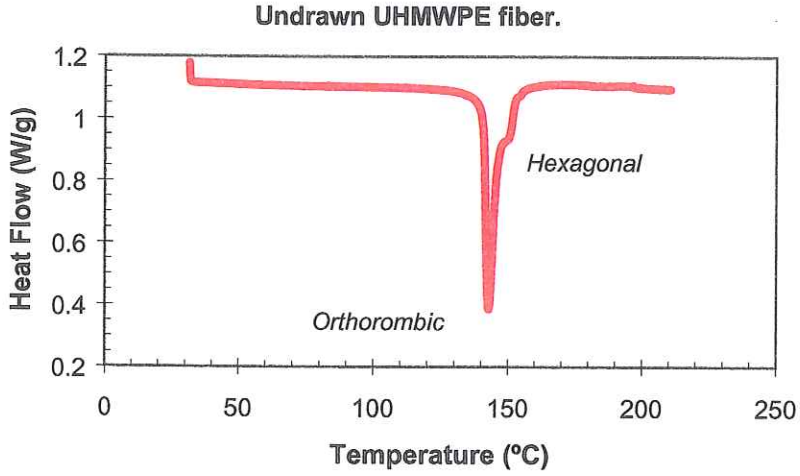

Figure 13. Typical DSC scan of an undrawn UHMWPE fiber at a heating rate of 1°C/min.

As can be seen from Figure 13 two melting endotherms can be detected. At approximately 142°C a large endotherm corresponding to the characteristic transition involving the melting of PE crystals within an orthorhombic unit cell is observed. Along with this, another endotherm is observed at 150°C, which corresponds to the transition of PE crystals within a hexagonal unit cell to the melt phase. The presence of this hexagonal phase as described in the literature is mainly associated with the presence of a highly oriented structure and is typically observed in samples processed under high pressure.

The differences in the drawing behavior and mechanical properties, observed within samples processed at different conditions, were initially thought to promote clear differences in the thermal behavior as well. The thermal response of samples treated in high-pressure CO_2 was compared to that of air-drawn samples at different drawing temperatures. The results are shown in Figures 14 and 15. From Figure 14 it can be seen that the thermal behavior of samples drawn in air is very temperature dependent. An apparent development of the hexagonal phase is present in these samples as judged by the considerable growth of the melting endotherm at 150°C with increasing the drawing temperature. In contrast, samples treated in high-pressure CO_2 appear to maintain their crystalline composition. These later samples show no difference in their thermal behavior over the entire range of processing temperatures.

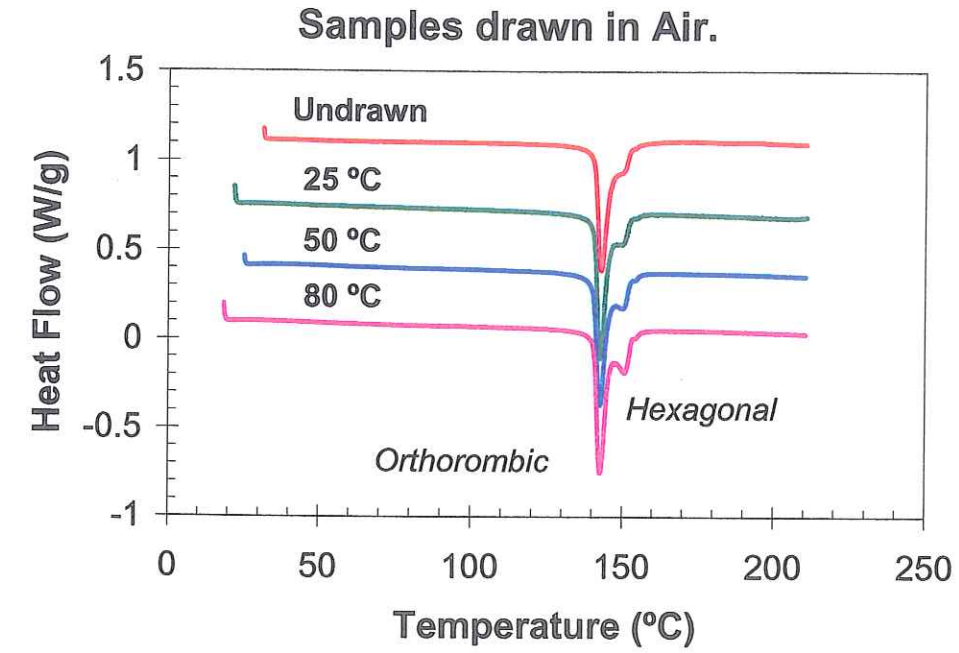

Figure 14. Thermal behavior of samples drawn in air at different temperatures.

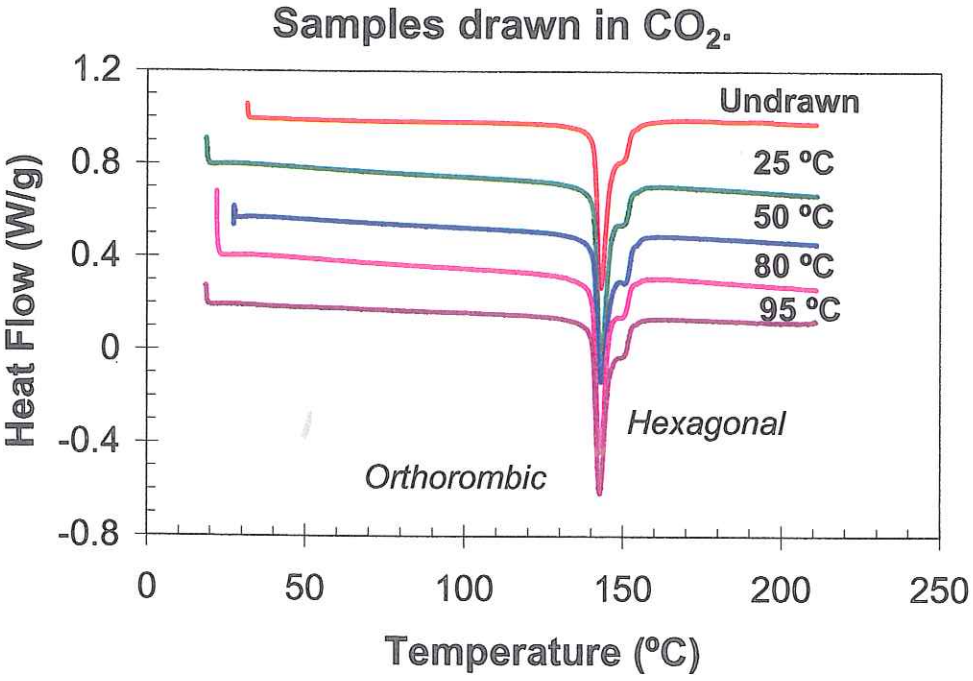

Figure 15. Thermal behavior of samples drawn in high-pressure CO_2 at different temperatures.

The composition of the crystalline phase was estimated by the ratio of the area under the curve of each melting endotherm. Results of this calculation are shown on Figures 16 and 17. These results verified the observation of the apparent development of a hexagonal phase in the air-drawn samples.

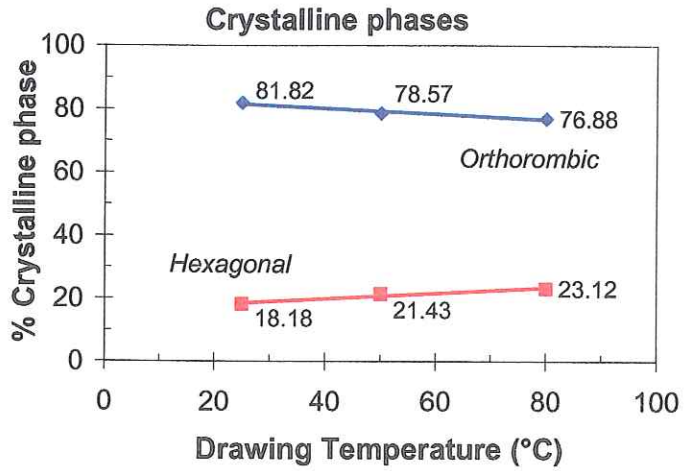

Figure 16. Crystalline phase composition of samples drawn in air at different temperatures.

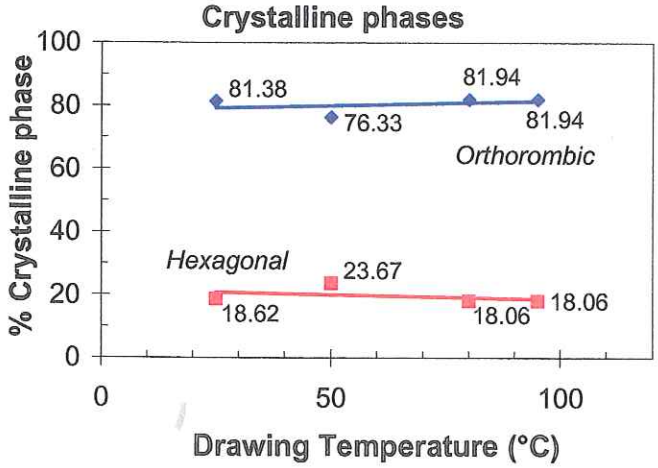

Figure 17. Crystalline phase composition of samples drawn in high-pressure CO_2 at different temperatures.

As can be seen from Figure 16, the amount of the apparent hexagonal phase increases almost 5% with increasing temperature. Again, as judged from Figure 17 the ratio of orthorhombic to hexagonal phase remains constant for the case of CO_2-drawn samples.

Along with the changes in the crystalline composition, DSC was used to estimate the increase in crystallinity due to the uniaxial deformation imposed in the samples. The total crystallinity of the samples was estimated by the ratio of the melting enthalpy of

both endotherms and the heat of fusion for PE (288.89 J/g). As can be seen in Figure 18 the crystallinty of samples treated in air increases considerably up to a value of 98% by increasing the processing temperature.

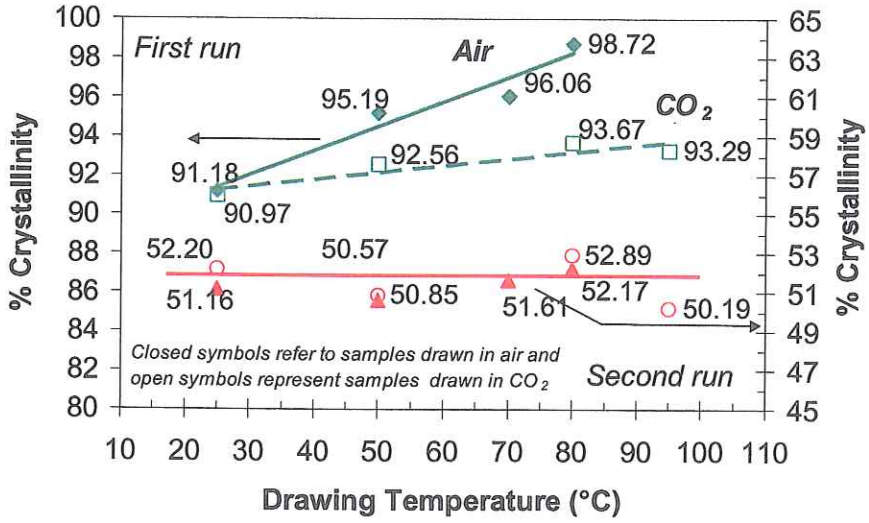

Figure 18. Crystallinity changes for samples drawn at different processing conditions.

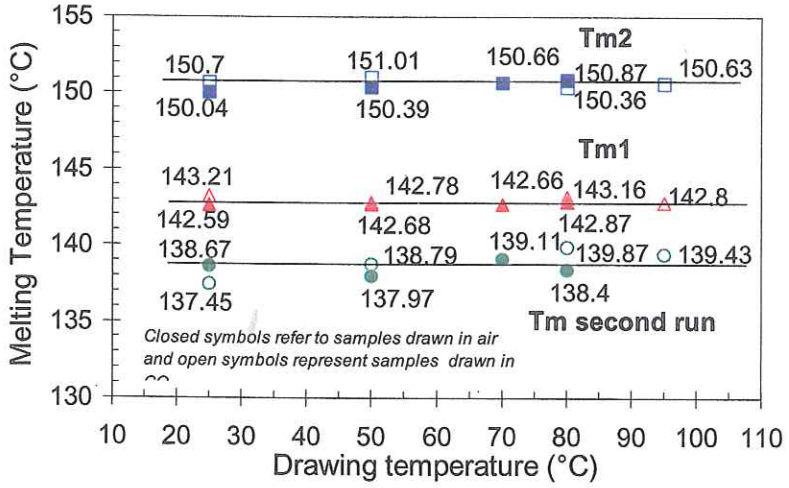

Figure 19. Melting temperatures for samples drawn at different processing conditions.

In contrast, the crystallinity of CO2-treated samples remains constant regardless of the processing conditions. Apparently from these results, smaller deformations were obtained in the presence of high-pressure CO_2, reducing the amount of strain-induced

crystallization. From this results it seem clear that CO_2 helps to maintain the integrity of the crystalline phase besides the fact that it does not interact with it. The presumable higher crystallinity observed in air-drawn samples correlates very well with the larger draw ratios observed experimentally, as described in the previous section.

No changes in the apparent melting points regardless of the processing conditions were observed as can be seen in Figure 19. The imposed deformation did not promote changes or alterations to the crystalline lamellae. In all cases a second run in the DSC show a broad melting point around 139°C showing that the highly orientation of the original sample is destroyed in the melting process. The crystallinity in these cases remains constant around 51% as shown in Figure 18.

Scanning Electron Microscopy (SEM)

A Scanning Electron Microscope model JEOL-CS-35 was employed to analyze the macroscopic morphology of the deformed materials. A filament voltage of 20kV was selected in all cases. SEM images were used to estimate and compare the amount of macroscopic damage created by the imposed deformation and its relation with the processing conditions.

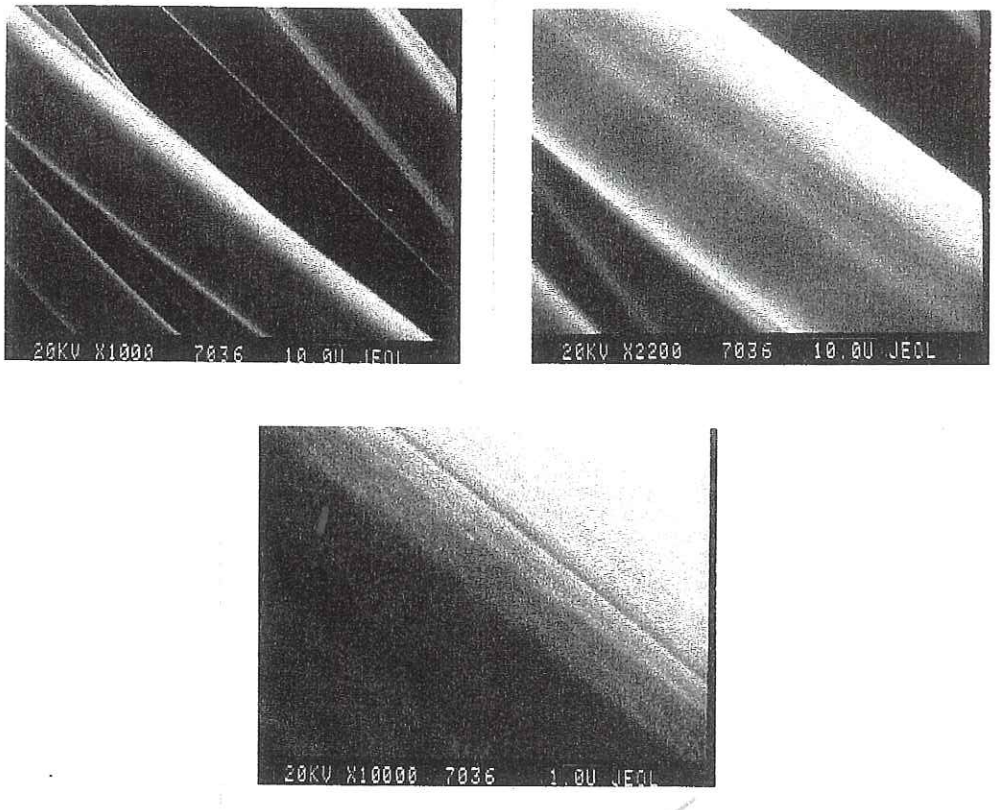

Figure 20. SEM images of undrawn UHMWPE samples.

As shown in Figure 20, the general morphology of an undrawn UHMWPE fiber is characterized by a considerably smooth surface, with no evident flaws even at higher magnifications. These factors arise as a consequence of the highly oriented structure of this sample. Fibers of 20-30μm in diameter with no significant size polidispersity characterize this material.

Samples drawn at different processing conditions were also compared in terms of their general morphology, as depicted in Figure 21. It can be seen from this figure that differences previously observed in terms of the mechanical properties and thermal behavior for air and CO_2 treated samples, did not appear to promote evident changes in terms of the macroscopic morphology.

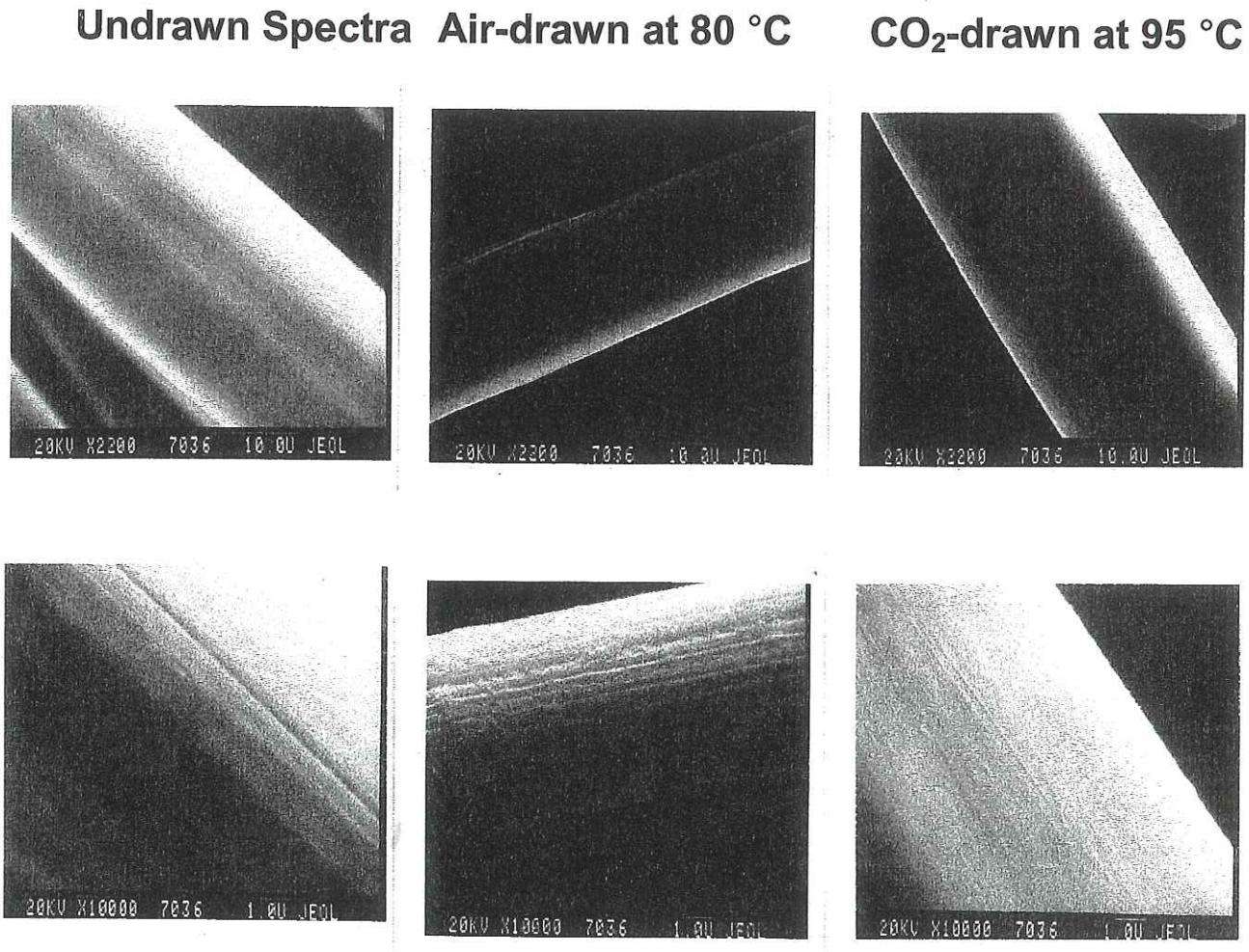

Figure 21. SEM images of UHMWPE fibers processed at different conditions.

The general morphology of samples treated at higher temperatures even in the presence of high-pressure CO_2 did not change too much with respect to that of the undrawn sample. The imposed deformation and in some cases the hydrostatic pressure have no effect in the smoothness of the material. All the materials appear to maintain their high orientation regardless of the processing conditions. This observation confirms that the differences previously observed, appear to act in a smaller length scale without promoting significant changes in the macroscopic morphology of the fiber.

Wide Angle X-ray Scattering (WAXS)

Wide-angle x-ray scattering (WAXS) experiments were done using a Statton camera device with an operating voltage of 40kV and a total current of 30mA under vacuum conditions. WAXS experiments were primarily employed both to corroborate the existence of the apparent hexagonal phase detected in the DSC and to estimate the effects of the deformation on the crystal integrity of the samples. The geometry of the measurements was such that the fibers were placed perpendicular to the direction of the beam. The scattering pattern of the undrawn UHMWPE fiber was compared to that of fibers drawn at different conditions. The results of some of the samples analyzed are presented in Figure 22.

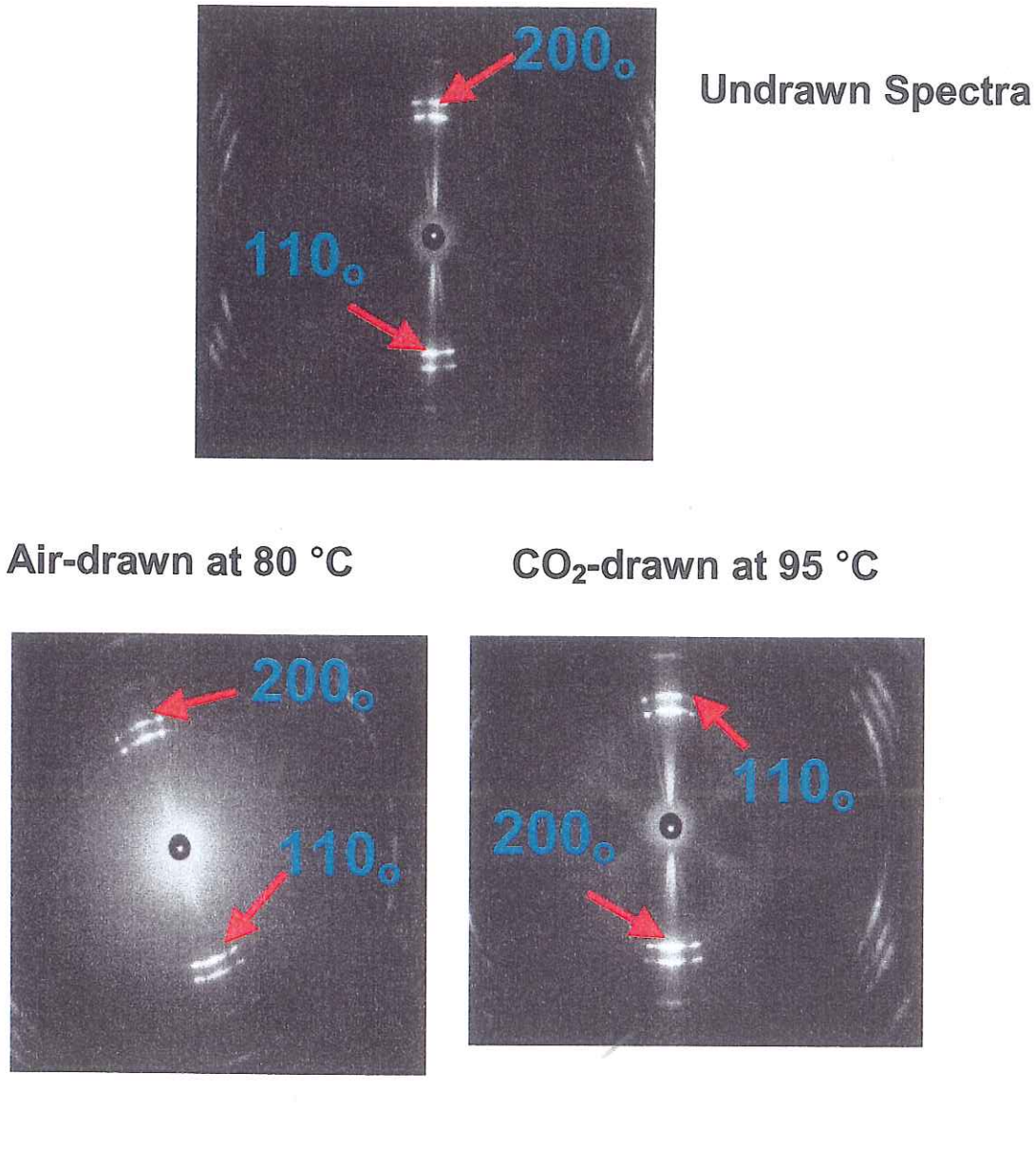

Figure 22. WAXS analysis of UHMWPE fibers drawn at different conditions.

From Figure 22 it is evident that all the samples present a highly oriented structure, in all the cases well-defined reflections were obtained. This actually facilitates the assignment of the planes observed experimentally. The strong reflections dominates completely the scattering pattern, almost no sign of an amorphous halo is present in any of the samples which corroborates the high values of crystallinity obtained by DSC.

As shown in Figure 22, two principal reflections were observed for the case of the undrawn sample. The first of these corresponds to the reflection of the 110_o plane from an orthorhombic unit cell, a reflection observed typically in PE. The other principal reflection is also assigned to the reflection of an orthorhombic unit cell, in this case the 200_o plane. No reflections were assigned to a hexagonal type of unit cell.

When comparing this scattering pattern with those of samples drawn at different conditions no significant changes were observed as shown in Figure 22. Regardless of the processing conditions exactly the same type of reflections were observed. Surprisingly, even for the sample treated in air at 80°C, which showed a large melting endotherm at 150°C in the DSC presumably corresponding to a hexagonal phase, no evidence of a hexagonal phase was obtained by WAXS.

There is no possibility of error in the assignment of the reflections. This can actually be verified in Table 3 and Figure 23. In Table 3 the experimentally observed d-spacings are compared with those of the typical unit cells found in UHMWPE. As can be seen, the observed reflections match exactly with the orthorhombic reflections. These results support the idea that the hexagonal phase is not present in the samples at ambient conditions.

Table 3. d-spacing of the observed reflections .

Sample	d-spacing (Å)	d-spacing (Å)
Theoretical orthorombic	4.10 **(110_o)**	3.70 **(200_o)**
Theoretical monoclinic	4.55 **(100_o)**	-
Theoretical hexagonal	4.33 **(100_o)**	-
Undrawn Spectra	4.101	3.703
Air-drawn at 80°C	4.136	3.740
CO_2-drawn at 95°C	4.128	3.720

Figure 23 shows the intensity-scattering angle graphs obtained in the different experiments. As mentioned earlier, this graph support the idea that at room temperature only the orthorhombic phase is present in these samples. It is easy to estimate that the scattering angles corresponding to the observed reflections, match exactly with the d-spacings of an orthorhombic type of unit cell.

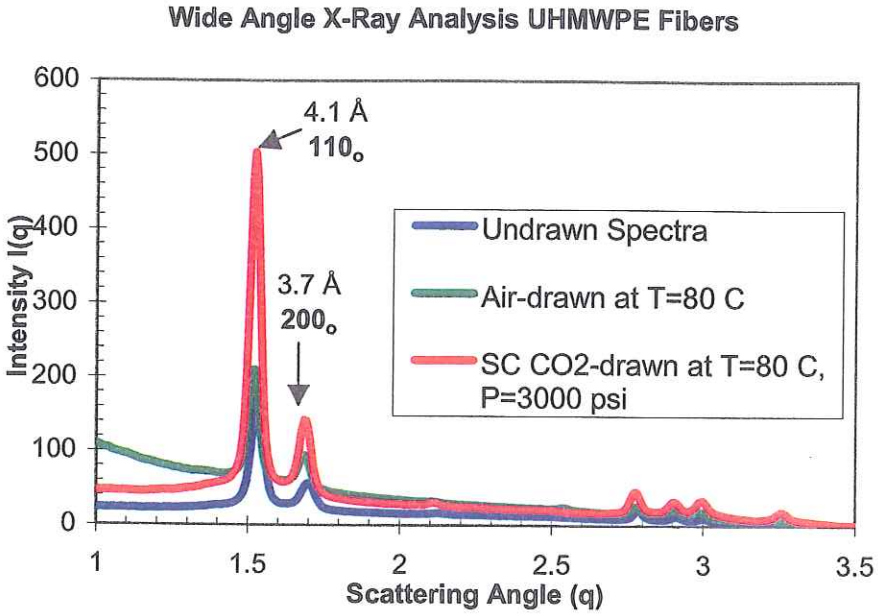

Figure 23. Intensity-scattering angle graphs of UHMWPE fibers drawn at different conditions.

DISCUSSION

As mentioned earlier, both the mechanical properties and drawing behavior of UHMWPE fibers is altered when the deformation is conducted in the presence of high-pressure CO_2. Apparently the supercritical CO_2 environment along with the hydrostatic pressure imposed help to maintain the integrity of this type of fibers, allowing them to deform up to a certain extent without changing the draw stress, which appears to be constant over the entire temperature range. The temperature dependence is completely suppressed when the experiment is done in the presence of supercritical CO_2. Modulus, strain at break and tensile strength are maintained unaltered when the fiber is drawn in CO_2, while significant weakening is observed for air-drawn samples with increasing temperature.

The thermal behavior of air-drawn samples is also dependent of the drawing temperature, as described in previous sections. A development of an apparent hexagonal phase along with a significant increase in the crystallinity is observed for the case these samples. Again, the presence of supercritical CO_2 appears to promote that the integrity of the crystalline phase in the sample remains unaltered regardless of the processing

conditions. In CO_2 experiments, no significant increase in crystallinity is observed, and the thermograms of samples deformed at different temperatures remain unchanged.

No significant changes in the general morphology are observed regardless of the processing conditions as suggested by SEM analysis. The high orientation remains unchanged in all the samples as confirmed by the strong reflections observed in WAXS. In contrast of what expected, the presence of the hexagonal phase in air-drawn samples deformed at higher temperatures was not confirmed by WAXS. An orthorhombic unit cell is present in all the samples, showing two strong reflections (110_o and 200_o), with no trace of the suggested hexagonal phase.

These results clearly suggest that the deformation in the presence of high-pressure CO_2 is different from that observed at ambient pressure. The high-pressure along with the presence of CO_2 promote significant differences in the deformation process, which reflect in the final thermal and drawing behavior.

Drawing in air appears to involve the deformation of an orthorhombic unit cell along the entire process. The macroscopic deformation imposed to the sample promotes some strain-induced crystallization, which is responsible for the increased crystallinity as detected by DSC. The macroscopic deformation is highly temperature dependent in this case, as judged by the considerable increase in the draw ratios for the case of air-drawn samples.

The addition of new crystals to the existing crystalline lamellae is restricted in this case due to the low mobility of chains within an orthorhombic unit cell, so these new crystals have basically two possibilities, either grow between the existent lamellae or as extended single chains, this later possibility being something specifically valid for PE. These two situations inevitably promote internal constraints in the sample. In any of these cases the newly born orthorhombic crystals will tend to expand to the more mobile hexagonal phase during heating, relaxing the stress imposed by the internal constraints before transforming into the melt phase. This explains the appearance of the melting endotherm of the hexagonal phase observed at 150°C for the case of air-drawn samples. At ambient conditions, however, no hexagonal phase is present and only the orthorhombic unit cell is present as confirmed by WAXS.

The deformation in the presence of high-pressure CO_2 appears to involve a crystal-crystal transformation, from the orthorhombic unit cell observed at room temperature to the more mobile hexagonal phase due to the high-pressure environment (3000 psi). It is well known that the mobility of the hexagonal phase is related with the degrees of freedom that a chain in this unit cell will have in terms of the rotations around the c-axis, but that the deformation along the chain backbone is somewhat restricted. If as suggested a hexagonal phase is formed in this case, lower macroscopic deformations are expected for these samples due to the imposed uniaxial deformation. This is actually in agreement with the lower draw ratios observed in this case with respect to the air-drawn samples.

The smaller macroscopic deformations in these cases restrict the amount of strain-induced crystallization, promoting that the crystallinity of samples treated in CO_2 do not change with increasing drawing temperature, something also confirmed by DSC. The appearance of the hexagonal phase due to the presence of high-pressure CO_2 also explains the observed increase in the processing temperature range. Since the hexagonal phase melt at a higher temperature, the deformation can be conducted at higher

temperatures without considerable softening. As mentioned before an increase of almost 30°C was observed when the deformation was done with supercritical CO_2.

In contrast with the case of air-drawn samples, in this case the newly born crystals can be added to the existing crystalline lamellae without promoting internal constraints into the sample, due to the high mobility of the hexagonal phase promoted by the high-pressure. Thus, no change in terms of the thermal behavior is expected for samples treated in supercritical CO_2 at different temperatures, something also confirmed experimentally by DSC. At the end of the experiment, when the pressure is released and the temperature is reduced, crystals within the sample will return to the original orthorhombic phase, and as described below, no internal constraints will be present. This explains the fact that only an orthorhombic phase is detected by WAXS in these samples at ambient conditions.

CONCLUSIONS

The drawing behavior of UHMWPE fibers (Spectra 900) in supercritical CO_2 ($scCO_2$) was compared to that in air at different temperatures. Samples drawn in air showed a considerable temperature dependence in their drawing properties. In contrast $scCO_2$-drawn samples showed a constant draw stress (≈290 MPa) and tensile strength (≈1500 MPa) over the entire temperature range. The existence of a hexagonal phase in the air-drawn samples was suggested by DSC by the appearance of a melting endotherm around 150°C with increasing drawing temperature. Along with these results, significant improvements in crystallinity were observed for these samples by increasing the processing temperature. WAXS results, however, suggested that no hexagonal phase was present in any of the samples regardless of the processing conditions. These results showed that the appearance of the high-temperature melting peak in DSC was due to the internally constrained manner in which air-drawn samples crystallize. In contrast, samples deformed in $scCO_2$ were able to crystallize and grow without internal constraints via a possible crystal-crystal transformation to a hexagonal unit cell. The existence of this hexagonal unit cell during deformation in $scCO_2$ is consistent with the lower draw ratios experimentally confirmed for these samples, as well as with the increased processing temperature up to a value of 110°C.

This document reports research undertaken at the U.S. Army Soldier and Biological Chemical Command, Soldier Systems Center, Natick, MA, and has been assigned No. NATICK/TR-03/003 in a series of reports approved for publication.

REFERENCES

1. Hobbs T. and Lesser A.J., Journal of Polymer Science. Part B: Polymer Physics, vol.37, 1881-1891, (1999).
2. Hobbs T. and Lesser A.J., Polymer, 41, 6223-6230, (2000).
3. Zachariades A.E. and Porter R.S., Journal of Applied Polymer Science, 24, 1371, (1979).
4. Lee D., Chen W., Yeh M. and Chen T., Polymer Engineering and Science, Mid-October, vol.35, No.19, (1995).
5. Tashiro K., Sasaki S. and Kobayashi M., Macromolecules, 29, 7460-7469, (1996).
6. Rastogi S., Kurelec L. and Lemstra P.J., Macromolecules, 31, 5022-5031, (1998).
7. Walsh T.F., Lee B.L. and Song J.W., Key Engineering Materials, vol.141-143, 367-382, (1998).
8. Kurelec L., Rastogi S., Meier R.J. and Lemstra P.J., Macromolecules, 33, 5593-5601, (2000).
9. Kuwabara K. and Horii F., Macromolecules, 32, 5600-5605, (1999).
10. Takayanagi M., Imada K., Nagai A. Tatsumi T. and Matsuo T., Journal of Polymer Scince. Part C, No.16, 867-876, (1967).
11. Peacock A. J., Handbook of Polyethylene. Structures, Properties and Applications, Marcel Dekker, Inc., (2000).